

Ni(III)/(IV) Bis(dicarbollide) as a Fast, Noncorrosive Redox Shuttle for Dye-Sensitized Solar Cells

Tina C. Li,^{†,‡} Alexander M. Spokoiny,^{†,§} Chunxing She,^{†,‡} Omar K. Farha,^{†,§} Chad A. Mirkin,^{*,†,§} Tobin J. Marks,^{*,†,‡} and Joseph T. Hupp^{*,†,‡,§}

Department of Chemistry, Argonne-Northwestern Solar Energy Research Center (ANSER), and International Institute for Nanotechnology, Northwestern University, 2145 Sheridan Road, Evanston, Illinois 60208

Received January 15, 2010; E-mail: j-hupp@northwestern.edu; t-marks@northwestern.edu; chadnano@northwestern.edu

The favorable energetics of dye-sensitized solar cell (DSC) constituents have advanced photoelectrochemical power conversion efficiencies to an impressive $\sim 11\%$.¹ However, the performance of DSCs based on the Γ^-/I_3^- redox couple has essentially plateaued, and additional component modifications have not advanced efficiency.² Indeed, the limitations placed on DSC dyes, semiconductors, and counter electrodes by Γ^-/I_3^- compatibility have presented a major challenge. DSC efficiency rests on a delicate balance of charge transport and recombination processes, with attempts to find redox shuttle alternatives to the Γ^-/I_3^- meeting limited success. To date, only a handful of cationic redox couples (e.g., Co(II/III)³ and Cu(I/II)⁴ complexes) and p-type semiconductors⁵ have functioned as effective redox mediators. While rapidly exchanging, outer-sphere redox couples such as ferrocene/ferrocenium (Fc/Fc^+) appear, a priori, promising for dyes with low overpotentials, rapid interception of injected electrons by Fc^+ leads to inadequate electron diffusion lengths and charge lifetimes.⁶

In searching for chemically robust and DSC-compatible redox couples, we focused on organometallic boron chemistry.⁷ Metallacarboranes,⁸ boron-based metallocene analogues, exhibit extraordinary chemical stability but simultaneously offer diverse derivatization options,⁹ suggesting diverse applications.¹⁰ Ni bis-(dicarbollide), featuring two η^5 -coordinated deboronated (nido-2) *o*-carborane **1** ligands (Figure 1a), readily undergoes multiple redox transformations involving net charges of -2 , -1 , and 0 , with Ni(II), Ni(III) (**3**), and Ni(IV) (**4**) oxidation states, respectively.¹¹ Species **3** and **4** exhibit high thermal stability (up to 300 °C), as judged by thermogravimetric analysis (see Supporting Information (SI), p S4). These properties make Ni (III)/(IV) bis(dicarbollides) attractive for DSC applications.

Here we report the implementation of Ni-based metallacarboranes **3** and **4** as a new, noncorrosive anionic redox shuttle for DSCs. The $\mathbf{3} \rightleftharpoons \mathbf{4}$ interconversion is a simple one-electron process, requiring suppression of the fast back-transfer of photoinjected electrons to complex **4**. This is accomplished by applying a barrier to the TiO_2 framework to slow charge transfer at the electrolyte interface. Previous DSC Fc/Fc^+ couple work showed that dark currents can be suppressed by TiO_2 surface passivation via conformal, Å-precise atomic layer deposition (ALD) of Al_2O_3 .^{12,13} We show here that the efficacious combination of the $\mathbf{3}/\mathbf{4}$ couple and TiO_2 ALD passivation yields DSC devices having impressively high efficiencies for these fast shuttles.

Although the potential of the $\mathbf{3}/\mathbf{4}$ couple lies ~ 140 mV negative of Fc/Fc^+ vs SCE (translating to a smaller potential difference between the dark electrode and quasi-Fermi level in the TiO_2), an

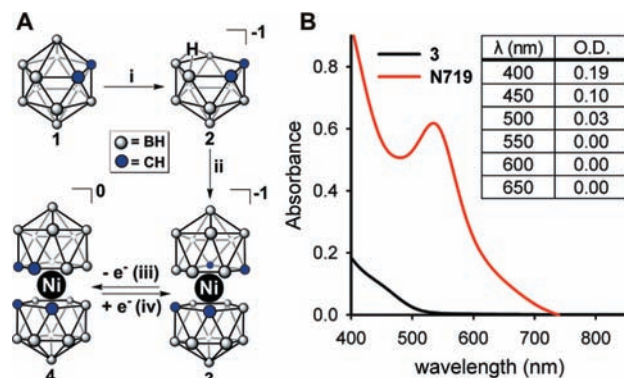


Figure 1. (a) Synthetic scheme: (i) NaOH, EtOH, reflux, then $\text{Me}_3\text{N}\cdot\text{HCl}$; (ii) 50% aqueous NaOH, $\text{NiCl}_2\cdot 6\text{H}_2\text{O}$, then Me_4NCl ; (iii) aqueous FeCl_3 or electrochemical oxidation; (iv) NaBH_4 , EtOH, or electrochemical reduction. (b) Optical absorption spectrum for a $5\ \mu\text{m}$ thick N719-sensitized nanoparticulate TiO_2 film (red) and adjusted spectrum for 0.10 M **3** (black) in acetonitrile, assuming a $5\ \mu\text{m}$ path length and 50% film porosity. Inset table shows electrolyte absorption.

open-circuit voltage (V_{oc}) almost three times greater than Fc/Fc^+ (580 mV vs 200 mV) is achieved using a mixture of reduced **3** (0.030 M) and oxidized **4** (1.8×10^{-3} M) in acetonitrile. Overall, the present DSCs exhibit power conversion efficiencies of 0.9% with *tert*-butylpyridine and TMABF₄ as solution additives, a significant advance over Fc/Fc^+ systems, which thus far have exhibited efficiencies of merely 0.01%.¹² The application of bis(dicarbollide) pairs to DSCs thus offers a new generation of fast redox shuttles which significantly out-perform previous metallocene studies.

Various shuttle concentrations were studied to determine the optimal electrolyte composition (Figure 2b), with the concentrations of the components, **3**, **4**, TMABF₄, and *tert*-butylpyridine, maintained at a fixed 50:3:10:50 ratio for all experiments. Higher short-circuit current density (J_{sc}) at low electrolyte concentrations are attributed primarily to the decreased local concentration of **4** and, consequently, the decreased electron interception by **4**. This is corroborated by the slight increase in V_{oc} observed at low concentrations of electrolyte, from 460 mV at 0.50 M **3** to 580 mV at 0.030 M **3**. Furthermore, improved light harvesting is due to the attenuation of competitive electrolyte absorption below 500 nm. For the $\mathbf{3}/\mathbf{4}$ redox couple, absorption is minimal for $\lambda \geq 500$ nm while the standard DSC dye N719 has $\lambda_{max} \approx 535$ nm, and thus the present cells exhibit good light harvesting. Figure 2c shows the incident photon-to-current conversion efficiency (IPCE) spectrum for a cell having 0.030 M **3** with a maximum of 11% at 535 nm, tracking the absorption spectrum of N719. Increasing the redox shuttle concentration to 0.30 M decreases the IPCE maximum to 9.0%, as indicated in Figure 2c. The Figure 2c inset reveals nearly

[†] Department of Chemistry, Northwestern University.

[‡] Argonne-Northwestern Solar Energy Research Center (ANSER), Northwestern University.

[§] International Institute for Nanotechnology, Northwestern University.

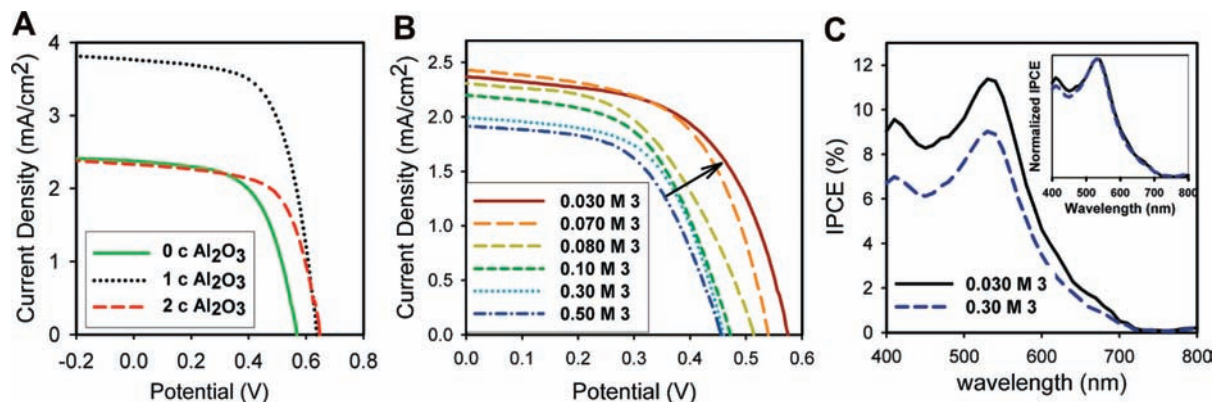


Figure 2. (a) J - V characteristics of DSCs containing **3** (0.030 M), **4** (1.8×10^{-3} M), TMAFB₄ (6.0×10^{-3} M), and *tert*-butylpyridine (0.036 M) with 0–2 cycles of ALD Al₂O₃ coverage of the TiO₂; (b) J - V characteristics with decreasing electrolyte concentration; (c) IPCE comparison of electrolyte containing 0.30 M (blue dotted) and 0.030 M (black solid) TMA-3 solutions (inset shows normalized IPCE spectra).

identical photoaction spectra by scaling the IPCE spectrum of the 0.30 M cell by 1.26 \times , indicating minor photon loss due to electrolyte absorption. This 21% IPCE loss is attributed to the 10-fold increase in redox shuttle concentration and is confirmed by a parallel decrease in J_{sc} , from 2.4 mA/cm² at 0.030 M to 1.9 mA/cm² at 0.30 M of **3**.

Thin insulating layers of large band gap MgO,¹⁴ ZrO₂,¹⁵ SrTiO₃,¹⁶ and Al₂O₃¹⁷ have been previously deposited on DSC TiO₂ photoelectrodes to tune interfacial charge dynamics. Electron interception by the electrolyte is considered to be the predominant power conversion pathway, assuming fast dye regeneration. With a physical barrier at the TiO₂/dye interface, charge leakage resulting from direct semiconductor–electrolyte contact is reduced, thus dramatically enhancing overall DSC performance. Using ALD, conformal Al₂O₃ growth is effectively achieved (~ 1.1 Å per ALD cycle) on the TiO₂ nanoparticle framework. Increased J_{sc} is believed to largely reflect passivation of surface states causing localization of electron density on the TiO₂ surface, since 1 Al₂O₃ ALD cycle deposits less than a monolayer.¹² Eliminating these defect sites impedes electron capture by the neighboring redox couple, thus reducing dark current. For each order of magnitude that charge interception is reduced, there is a $\gamma \cdot 59$ mV gain in photovoltage, where the diode quality factor γ is usually 1.0–1.5, assuming electron transfer from the conduction band.¹⁸ This effect is confirmed by the increase in V_{oc} from 580 mV to 640 mV with 1 cycle of Al₂O₃ passivation, yielding $J_{sc} = 3.76$ mA/cm² and an overall power conversion efficiency of 1.5%. Further Al₂O₃ deposition hinders current collection, reducing J_{sc} by $\sim 50\%$ for 2 Al₂O₃ cycles. This drop in current may indicate the suppression of electron injection, resulting from the insulating Al₂O₃ barrier. With 2 ALD cycles, the TiO₂ surface is completely coated with Al₂O₃. Thus, beyond 1 deposition cycle, charge interception is no longer reduced primarily by trap state passivation but by increased distance between photoinjected electrons and **4**. Retardation of electron interception is apparent in the successive photovoltage increase with increasing Al₂O₃ coverage, but optimal performance is achieved at only 1 ALD cycle due to its relatively high J_{sc} .

The open-circuit voltage decay technique was next used to probe the kinetics of interception by the electrolyte.¹⁹ Comparisons of the 3/4 redox couple with I[−]/I₃[−] and Fc/Fc⁺ are shown in Figure 3a with potentials adjusted to the Fc/Fc⁺ solution for reference.¹² From the charge lifetimes vs potential plots, interception appears to be $\sim 10^3 \times$ slower than for Fc/Fc⁺, but almost 100 \times faster than I[−]/I₃[−]. Slower 3/4 shuttle kinetics are expected since the Ni(IV) \rightarrow Ni(III) reduction requires dicarbollide rotation from a *cis* \rightarrow *trans* conformation (see Figure

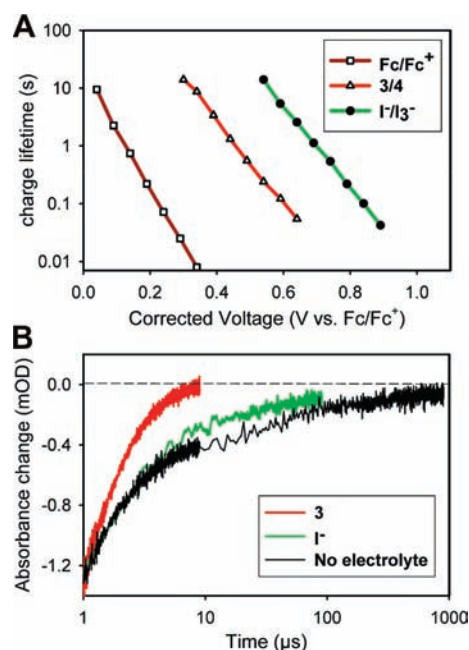


Figure 3. (a) Charge lifetime plots from V_{oc} decay for different redox shuttles with 1 ALD cycle of Al₂O₃ on the TiO₂ nanoparticle framework. (b) Ground-state recovery kinetics of N719 adsorbed on TiO₂ films probed at 500 nm after excitation at 532 nm. Films were soaked in 0.03 M of **3** and I[−] solutions.

1a). This in turn creates a larger activation barrier for the reduction of **4** than for Fc⁺, translating to a slower interception rate. However, compared to I[−]/I₃[−], the 3/4 kinetics are fast, involving facile **3** \rightarrow **4** one-electron transfer, thereby allowing efficient dye regeneration, and opening the possibility of incorporating DSC dyes with less positive ground state potentials than widely used “N719”. Nevertheless, to make full use of the new shuttle, it will be necessary to turn to photoelectrode materials and architectures displaying faster electron transport and collection;²⁰ the observed modest IPCE values indicate, with nanoparticulate TiO₂ as the photoelectrode material, significant deleterious competition from electron interception by **4**.

Transient absorption spectroscopy confirms that the remarkable performance of 0.030 M **3** results from fast dye regeneration. Thus, Figure 3b compares N719 ground-state recovery kinetics, probed at 500 nm, for 0.030 M **3**, 0.030 M 1-butyl-3-methylimidazolium iodide, and pure solvent. Dye regeneration in the absence of electrolyte (recombination) occurs in tens of microseconds and

slower, agreeing well with literature data.²¹ Dye regeneration by **3** occurs in $<2 \mu\text{s}$ ($t_{1/2}$), slightly faster than that by Γ^- . Remarkably, regeneration by **3** is 10–100× faster than recombination, thus affording a regeneration yield of $\geq 90\%$.

In addition to efficient dye regeneration kinetics, the **3/4** shuttle has a fast rate of electron exchange at the counter electrode, minimizing voltage losses.²² Platinized counter electrodes are typically used in DSCs since Pt efficiently catalyzes the $\text{I}_3^- \rightarrow \Gamma^-$ reduction.²³ However, Au and carbon have also been used as alternative cathode materials for cobalt-based shuttles.⁴ Unlike the Γ^-/I_3^- redox mediator, the **3/4** shuttle is stable with respect to other conductive metals, and in fact, replacing Pt with Ag or Au at the counter electrodes gives similar or enhanced photovoltaic characteristics. Thus, a Au counter electrode gives the highest J_{sc} and fill factor in this study (see SI, p S6), most likely due to the greater electrode reflectivity, increasing the optical path through the cell. The performance with Ag was also explored and shown to follow similar trends with ALD modification. Other cost-efficient materials are being explored.

In summary, the **3/4** shuttle is shown to be a promising, noncorrosive DSC shuttle with good solubility and redox properties. In contrast to Co and Cu based shuttles, **4** is neutrally charged and therefore does not appreciably adsorb on the TiO_2 photoanode. Additionally, the **3/4** shuttle exhibits slower kinetics than Fc/Fc^+ and therefore a slower rate of electron interception by the electrolyte. Marked suppression of dark currents is achieved, with the kinetically slower **3/4** reaching photovoltages of 640 mV after Al_2O_3 deposition, significantly higher than the case for the Fc/Fc^+ couple, and enhancing current densities by 2–3× with only 1 Al_2O_3 ALD cycle. Furthermore, Au is shown to be an attractive alternative counter electrode in these cells, providing superior current densities and fill factors. The remarkable inertness of **3/4** toward Ag metal may be beneficial for large-scale DSC fabrication, if Ag contacts are used. This novel fast, one-electron transfer system opens the possibility for new dyes and frameworks to be incorporated into DSCs, with dicarbollide ligands readily tunable to alter the shuttle charge transfer characteristics.

Acknowledgment. J.T.H. and T.J.M. gratefully acknowledge the support of BP Solar. J.T.H. also thanks the U.S. DOE Office of Science (Grant No. DE-FG02-87ER13808) and NU-NSEC for funding. T.J.M. acknowledges the support of the Energy Frontier Research center (DE-SC0001059) at the ANSER Center of Northwestern University. C.A.M. acknowledges the DOE Office of Basic Energy Sciences (Award No. DE-SC0000989) for support via the NU Nonequilibrium Energy Research Center. He is also grateful for support from the Army Research Office.

Supporting Information Available: Experimental data, solar cell fabrication and characterizations, CV, TGA, current transients between 1/10 to 1 sun illuminations, and J – V characteristics for varying electrolyte concentrations, alternative counter electrodes and with ALD Al_2O_3 modification. This material is available free of charge via the Internet at <http://pubs.acs.org>.

References

- (1) (a) Grätzel, M. *Inorg. Chem.* **2005**, *44*, 6841. (b) Chiba, Y.; Islam, A.; Watanabe, Y.; Komiya, R.; Koide, N.; Han, L. Y. *Jpn. J. Appl. Phys. Pt. 2* **2006**, *45*, L638–L640. (c) Boschloo, G.; Hagfeldt, A. *Acc. Chem. Res.* **2009**, *42*, 1819–1826.
- (2) (a) Hamann, T. W.; Jensen, R. A.; Martinson, A. B. F.; Ryswyk, H. V.; Hupp, J. T. *Energy Environ. Sci.* **2008**, *1*, 66–78. (b) Martinson, A. B. F.;

- Hamann, T. W.; Pellin, M. J.; Hupp, J. T. *Chem.—Eur. J.* **2008**, *14*, 4458–4467.
- (3) (a) Cameron, P. J.; Peter, L. M.; Zakeeruddin, S. M.; Grätzel, M. *Coord. Chem. Rev.* **2004**, *248*, 1447–1453. (b) Cazzanti, S.; Caramori, S.; Argazzi, R.; Elliot, C. M.; Bignozzi, C. A. *J. Am. Chem. Soc.* **2006**, *128*, 9996–9997. (c) Sapp, S. A.; Elliott, C. M.; Contado, C.; Caramori, S.; Bignozzi, C. A. *J. Am. Chem. Soc.* **2002**, *124*, 11215–11222.
- (4) Hattori, S.; Wada, Y.; Yanagida, S.; Fukuzumi, S. *J. Am. Chem. Soc.* **2005**, *127*, 9648–9654.
- (5) (a) Yum, J.-H.; Chen, P.; Grätzel, M.; Nazeeruddin, M. K. *ChemSusChem* **2008**, *1*, 699–707. (b) Li, B.; Wang, L.; Kang, B.; Wang, P.; Qiu, Y. *Sol. Energy Mater. Sol. Cells* **2006**, *90*, 549–573. (c) Bach, U.; Lupo, D.; Comte, P.; Moser, J. E.; Weissörtel, F.; Salbeck, J.; Spreitzer, H.; Grätzel, M. *Nature* **1998**, *395*, 583–585. (d) Yanagida, S.; Yu, Y.; Manseki, K. *Acc. Chem. Res.* **2009**, *42*, 1827–1838.
- (6) Gregg, B. A.; Pichot, F.; Ferrere, S.; Fields, C. L. *J. Phys. Chem. B* **2001**, *105*, 1422–1429.
- (7) Siebert, W. *Advances in Boron Chemistry*; UK, 1997.
- (8) Grimes, R. N. *Carboranes*; Academic Press: New York, 1970.
- (9) (a) Warren, L. F.; Hawthorne, M. F. *J. Am. Chem. Soc.* **1970**, *92*, 1157–1173. (b) Farha, O. K.; Spokoyny, A. M.; Mulfort, K. L.; Hawthorne, M. F.; Mirkin, C. A.; Hupp, J. T. *J. Am. Chem. Soc.* **2007**, *129*, 12680–12681. (c) Wade, K. *Nat. Chem.* **2009**, *1*, 92. (d) Spokoyny, A. M.; Reuter, M. G.; Stern, C. L.; Ratner, M. A.; Seideman, T.; Mirkin, C. A. *J. Am. Chem. Soc.* **2009**, *131*, 9482–9483. (e) Jude, H.; Disteldorf, H.; Fischer, S.; Wedge, T.; Hawkrige, A. M.; Arif, A. M.; Hawthorne, M. F.; Muddiman, D. C.; Stang, P. J. *J. Am. Chem. Soc.* **2005**, *127*, 12131–12139. (f) Dash, B. P.; Satapathy, R.; Maguire, J. A.; Hosmane, N. S. *Org. Lett.* **2008**, *10*, 22247–22250. (g) Mueller, J.; Base, K.; Michl, J. *J. Am. Chem. Soc.* **1992**, *114*, 9721–9722.
- (10) (a) Hawthorne, M. F.; Maderna, A. *Chem. Rev.* **1999**, *99*, 3421–3434. (b) Plešek, J. *Chem. Rev.* **1992**, *92*, 269–278. (c) Yang, X.; King, W. A.; Sabat, M.; Marks, T. J. *Organometallics* **1993**, *12*, 4254–4258. (d) Crowther, D. J.; Swenson, D. C.; Jordan, R. F. *J. Am. Chem. Soc.* **1995**, *117*, 10403–10404. (e) Hawthorne, M. F.; Zink, J. I.; Skelton, J. M.; Bayer, M. J.; Liu, C.; Livshits, E.; Baer, R.; Neuhauser, D. *Science* **2004**, *303*, 1849–1851. (f) Shen, H.; Xie, Z. *Chem. Commun.* **2009**, 2431–2445. (g) Planas, J. G.; Viñas, C.; Teixidor, F.; Comas-Vives, A.; Ujaque, G.; Lledós, A.; Light, M. E.; Hursthouse, M. B. *J. Am. Chem. Soc.* **2005**, *127*, 15976–15982. (h) Abram, P. D.; Ellis, D.; Rosair, G. M.; Welch, A. J. *Chem. Commun.* **2009**, 5403–5405. (i) Armstrong, A. F.; Lebert, J. M.; Brennan, J. D.; Valliant, J. F. *Organometallics* **2009**, *28*, 2986–2992. (j) Olejniczak, A. B.; Mucha, P.; Gruner, B.; Lesnikowski, Z. L. *Organometallics* **2007**, *26*, 3272–3274. (k) Cíglér, P.; Kozisek, M.; Rezáčová, P.; Brynda, J.; Otwinowski, Z.; Pokorná, J.; Plešek, J.; Grüner, B.; Dolecková-Maresová, L.; Máša, M.; Sedláček, J.; Bodem, J.; Kráuslich, H.-J.; Král, V.; Konvalinka, J. *Proc. Natl. Acad. Sci. U.S.A.* **2005**, *102*, 15394–15399. (l) Law, J. D.; Brewer, K. N.; Herbst, R. S.; Todd, T. A.; Wood, D. J. *Waste Management* **1999**, *19*, 27–37.
- (11) Hawthorne, M. F.; Dunks, G. B. *Science* **1972**, *178*, 462–471.
- (12) Hamann, T. W.; Farha, O. K.; Hupp, J. T. *J. Phys. Chem. C* **2008**, *112*, 19756–19764.
- (13) (a) Standridge, S. D.; Schatz, G. C.; Hupp, J. T. *Langmuir* **2009**, *25*, 2596–2600. (b) Guo, J.; She, C.; Lian, T. *J. Phys. Chem. C* **2007**, *111*, 8979–8987.
- (14) Taguchi, T.; Zhang, X.-T.; Sutanto, I.; Tokuyoshi, K.-I.; Rao, T. N.; Watanabe, H.; Nakamori, T.; Uragami, M.; Fujishima, A. *Chem. Commun.* **2003**, 2480–2481.
- (15) (a) Palomares, E.; Clifford, J. N.; Haque, S. A.; Lutz, T.; Durrant, J. R. *J. Am. Chem. Soc.* **2003**, *125*, 475–482. (b) Li, T. C.; Góes, M. S.; Fabregat-Santiago, F.; Bisquert, J.; Bueno, P. R.; Prasittichai, C.; Hupp, J. T.; Marks, T. J. *J. Phys. Chem. C* **2009**, *113*, 18385–18390.
- (16) Diamant, Y.; Chen, S. G.; Melamed, O.; Zaban, A. *J. Phys. Chem. B* **2003**, *107*, 1977–1981.
- (17) (a) Fabregat-Santiago, F.; García-Cañadas, J.; Palomares, E.; Clifford, J. N.; Haque, S. A.; Durrant, J. R.; Garcia-Belmonte, G.; Bisquert, J. *J. Appl. Phys.* **2004**, *96*, 6903–6907. (b) Palomares, E.; Clifford, J. N.; Haque, S. A.; Lutz, T.; Durrant, J. R. *Chem. Commun.* **2002**, 1464–1465.
- (18) (a) O'Regan, B. C.; Scully, S.; Mayer, A. C.; Palomares, E.; Durrant, J. J. *J. Phys. Chem. B* **2005**, *109*, 4616–4623. (b) Law, M.; Greene, L. E.; Radenovic, A.; Kuykendall, T.; Liphardt, J.; Yang, P. *J. Phys. Chem. B* **2006**, *110*, 22652–22663.
- (19) Zaban, A.; Greenshtein, M.; Bisquert, J. *ChemPhysChem* **2003**, *4*, 859–864.
- (20) (a) Martinson, A. B. F.; Góes, M. S.; Fabregat-Santiago, F.; Bisquert, J.; Pellin, M. J.; Hupp, J. T. *J. Phys. Chem. A* **2009**, *113*, 4015–4021. (b) Martinson, A. B. F.; Elam, J. W.; Liu, J.; Hupp, J. T.; Pellin, M. J.; Marks, T. J. *Nano Lett.* **2008**, *8*, 2862–2866.
- (21) Clifford, J. N.; Palomares, E.; Nazeeruddin, M. K.; Grätzel, M.; Durrant, J. R. *J. Phys. Chem. C* **2007**, *111*, 6561–6567.
- (22) Peter, L. M. *J. Phys. Chem. C* **2007**, *111*, 6601–6612.
- (23) (a) Wang, M.; Anghel, A. M.; Marsan, B.; Ha, N.-L.; Pootrakulchote, N.; Zakeeruddin, S. M.; Grätzel, M. *J. Am. Chem. Soc.* **2009**, *131*, 15976–15977. (b) Bay, L.; West, K.; Winther-Jensen, B.; Jacobsen, T. *Sol. Energy Mater. Sol. Cells* **2006**, *90*, 341–351.

JA100396N